The Design, Synthesis, and Evaluation of Profluoracil: A Small Molecule Dihydrofolate Reductase Inhibitor for Psoriasis Treatment

Lucas Rodriguez Chiappetta

North Carolina School of Science and Mathematics

1219 Broad Street

Durham, NC 27705

Abstract

Psoriasis is a chronic inflammatory skin disease that significantly impacts quality of life, causing both psychological and physical distress. Classical dihydrofolate reductase (DHFR) inhibitors, such as methotrexate and pemetrexed, have provided effective treatment for the condition; however, cellular resistance and hepatotoxicity limit their long-term usability. Unlike classical inhibitors, nonclassicals do not rely on active transport to enter a cell, bypassing common cellular resistance mechanisms. This project investigates the development of profluoracil: a less toxic, higher-affinity nonclassical inhibitor that incorporates a propargyl-linked fluorinated uracil scaffold. Propargyl-linked fluorouracil derivatives can exhibit high affinity for the DHFR binding site while avoiding the need for classical folate mimics—whose structures inherently cause toxic effects. Using Schrödinger's *Maestro Suite* for computational design and testing, profluoracil was discovered and then synthesized via a Sonogashira cross-coupling reaction. The compound was characterized by TLC analysis, and subsequently, inhibition of DHFR by profluoracil was evaluated relative to a methotrexate control, exhibiting a peak inhibition of 85% in the low nanomolar range. Results from an *Escherichia coli* cytotoxicity assay indicate that profluoracil demonstrates lower toxicity than methotrexate at high nanomolar to low micromolar concentrations. Preliminary testing suggests that profluoracil exhibits comparable—or possibly greater—potency than methotrexate, along with fewer side effects, offering a more effective, less toxic, nonclassical alternative to existing DHFR inhibitors.

1 Introduction

1.1 Psoriasis Background

Psoriasis is a chronic autoimmune disorder that affects approximately 125 million people worldwide, accounting for around 3% of the global population. The disease is characterized by thickened, inflamed, and scaly patches that often itch and burn **[Figure 1]**. Psoriasis treatment is challenging—topical ointments are pungent and tedious to apply to developing breakouts. Additionally, oral therapeutics produce harmful side effects like liver and immune system damage. Psoriasis severely impairs quality of life, causing physical discomfort and psychological distress; patients report lowered self-image and reduced confidence as a result of the disease [1]. Due to its cyclical nature, individuals with psoriasis may experience flare-ups lasting weeks or months, followed by periods of remission. These flare-ups are commonly triggered by infection, stress, or adverse reactions to medication. *Streptococcus* infections often introduce disease activity, while lithium and NSAID medications can heighten its prevalence [2]. At its core, psoriasis is driven by an overactive immune system, in which keratinocytes—cells that trigger inflammation—play a crucial role in its development and progression. When activated, keratinocytes release a variety of signaling molecules, including cytokines, in response to immune stimuli. This signaling creates a ripple effect, with keratinocytes proliferating rapidly, leading to epidermal thickening and the formation of characteristic patches [3–4]. Given its impact on mental health and the limitations of current treatment, inhibiting specific targets whose function promotes cellular proliferation is a crucial area for the development of potent therapeutics [5].

Figure 1. Psoriasis on the back showing characteristic patches. Image accessed from *Psoriasis of the Back* in October 2025, Wikipedia [6].

1.2 Function of Dihydrofolate Reductase Inhibition

Dihydrofolate reductase (DHFR) is an ubiquitous enzyme found in all living organisms. It plays a crucial role in one-carbon metabolism, a series of reactions that deliver one-carbon units to various molecules, such as lipids, amino acids, and nucleic acids **[Figure 2]**.

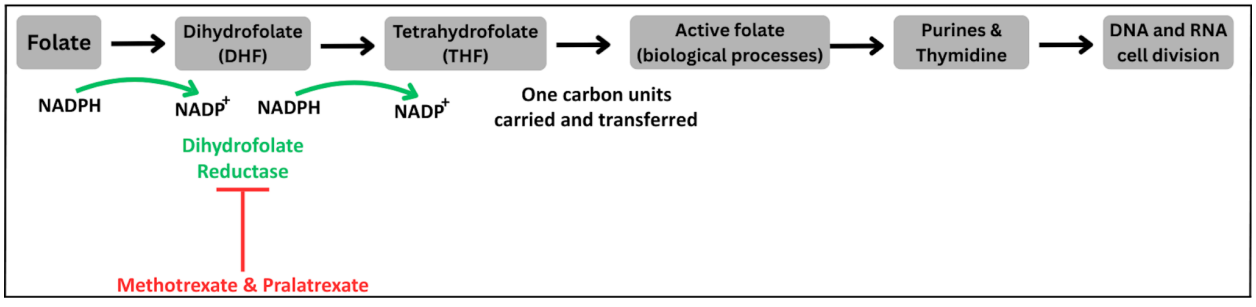

Figure 2. Simple schematic representation of one-carbon metabolism highlighting dihydrofolate reductase (DHFR) in the reduction of dihydrofolate (DHF) to tetrahydrofolate (THF). Red text indicates DHFR inhibitors, which disrupt the progression of one-carbon metabolism; green arrows indicate DHFR-catalyzed reactions. Image created by student researcher using Canva, 2025.

DHFR catalyzes the reduction of dihydrofolate (DHF) to tetrahydrofolate (THF) using NADPH as a cofactor. THF serves as a carrier of one-carbon units required for the synthesis of purine and thymidylate, precursors of DNA replication. As a result, inhibiting dihydrofolate reductase disrupts nucleotide synthesis, slowing DNA replication and preventing uncontrolled cell proliferation. Ultimately, this leads to cell death and apoptosis in rapidly dividing cells [7]. In psoriasis, the pathogenesis is characterized by hyperproliferation of keratinocytes; thus, DHFR inhibition offers an appealing strategy to counteract this process. By preventing the formation of THF, DHFR inhibition reduces nucleotide synthesis, limiting DNA replication and consequently, keratinocyte proliferation and the progression of psoriasis [1, 5, 8–9].

1.3 Classical and Nonclassical Dihydrofolate Reductase Inhibition

Dihydrofolate reductase inhibitors are categorized into two types: classical and nonclassical antifolates **[Figure 3]**. Classical inhibitors, such as methotrexate (MTX), consist of a pterin ring, aromatic ring (specifically a p-aminobenzoic ring in MTX), and a charged glutamate tail. These compounds mimic the structure of dihydrofolate, the natural substrate of DHFR, allowing competitive binding to the enzyme's active site. Specifically, when bound to human dihydrofolate reductase (hDHFR), these molecules participate in both hydrogen bonding and hydrophobic interactions, rendering them remarkably potent.

Classical inhibitors are highly polar, which prevents them from passing through the cell membrane by passive diffusion; therefore, they require the reduced folate carrier (RFC) to enter. Efflux pumps—transport proteins that move toxic compounds out of cells—contribute to cellular resistance mechanisms; their overexpression often expels drugs such as methotrexate from cells, preventing them from reaching their targets. Furthermore, alterations in drug uptake can lead to cellular resistance; fewer drug molecules enter the cell, requiring higher doses to achieve the same effect, thus increasing toxic effects.

In terms of inhibition and efficacy, classicals outperform other candidates; however, their success is hindered by toxicity. Specifically, these drugs exhibit considerable amounts of hepatotoxicity, causing both acute and chronic liver damage. Even low doses of these antifolates, when

administered over prolonged periods, can have adverse effects, raising concerns about long-term use [1, 5–7, 10–12].

Alternatively, nonclassical antifolates—such as propargyl-linked antifolates (PLAs), trimethoprim, 1,3-diamino-7H-pyrrol[3,2-f] quinazoline derivatives—are structurally different from their classical counterparts. Nonclassical inhibitors replace the aminobenzoic acid and glutamic acid components with lipophilic replacements. The lipophilic nature, combined with the absence of charged rings present in classical antifolates, facilitates passive diffusion. They do not have to rely on an RFC to transport across the cell, which decreases the likelihood of efflux or transporter resistance. Although structurally smaller, nonclassicals exhibit high DHFR potency. Nonclassical structures promote favorable hydrogen bonding and pi–pi stacking interactions with key amino acids within the DHFR active site. Some existing nonclassicals, such as trimetrexate, a common chemotherapy agent, exhibit IC_{50} values that are significantly lower than those of methotrexate [13]. Additionally, nonclassical inhibitors avoid common mechanisms that promote drug accumulation in healthy cells, thereby reducing overall toxicity [1, 8–9, 13–15].

1.4 Propargyl-linked Antifolates for Safer Psoriasis Treatment

New nonclassical antifolates targeting DHFR have been synthesized and tested in recent years, with propargyl-linked antifolates (PLAs) emerging as a particularly promising subgroup **[Figure 4]**. PLAs show potential due to their smaller structures and passive diffusion mechanisms, which reduce susceptibility to cellular resistance and facilitate facile synthetic routes. Their charge distributions and lipophilicity further minimize recognition and expulsion by efflux pumps. Recently tested propargyl-linked antifolates exhibit exceptional nanomolar potency, relative to both classical and nonclassical treatment, with reported IC_{50} values in the low nanomolar range [7]. The propargyl linker's extended structure promotes favorable interactions with key residues in the DHFR active site, resulting in stronger binding. Despite these advancements, many existing nonclassicals still exhibit limited efficacy and significant toxicity; thus, the continued development of safer, higher-affinity DHFR inhibitors is necessary. [7–9, 15–17].

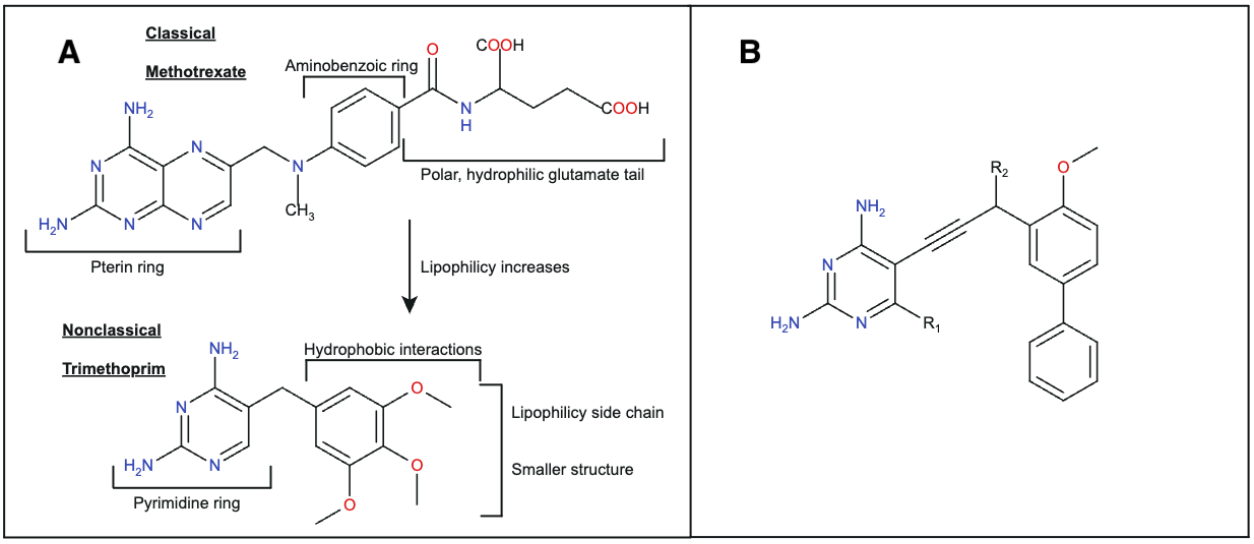

Figure 3. A) Comparison of classical (methotrexate) and nonclassical (trimethoprim) antifolate properties. Image created by student researcher using Marvin Chemical Drawing, 2025. **B)** Standard propargyl-linked antifolate. Image created by student researcher using Marvin Chemical Drawing, 2025.

1.5 Specific Aim

This project aims to design, synthesize, and evaluate a higher affinity, lower cellular resistance, small molecule dihydrofolate reductase (DHFR) inhibitor that exhibits reduced side effects relative to various nonclassical antifolates for the treatment of psoriasis.

2 Methodology

Evaluation of potential DHFR inhibitors proceeded in three stages: computational design, including docking of known and discovered compounds; synthesis of the most promising candidate based on computational testing; and *in vitro* inhibition and cytotoxicity testing of the synthesized compound.

2.1 Computational Design

Computational design was split into two stages: docking known inhibitors, followed by docking potential inhibitors. All computational design and modeling were performed in Schrödinger's *Maestro Suite* using a crystal structure of human dihydrofolate reductase (PDB:5SDB) **[Figure 4]**. Stage one included the design, preparation, and docking of existing classical and nonclassical

antifolates to human dihydrofolate reductase (e.g., methotrexate, premetrexed, pralatexate, etc.). These known compounds provided insight into the structures of potent inhibitors and served as benchmarks for binding and pharmacokinetic comparison with potential inhibitors. Stage two involved the development, preparation, and docking of potential drug candidates, including both purine and fluorouracil models. Initial docking tests were performed using purine structures; ~50 of these structures were designed with different linkers and tails (e.g., an ether linker with a glutamate tail) to facilitate favorable interactions while maintaining a smaller structure. The second round of discovered nonclassicals was –iodo and –bromo compounds linked to 5–Fluoro–1–propargyl-uracil. Around ~12 of these simpler structures were designed, prepped, and tested; results were stored and compared to both known inhibitors and the earlier purine structures. The best candidates, as determined by docking scores, were selected for further analysis. "QikProp," a Schrödinger tool that measures pharmacokinetic properties, was used to run simulations on these candidates and compare the results with those of known inhibitors [7, 14, 16].

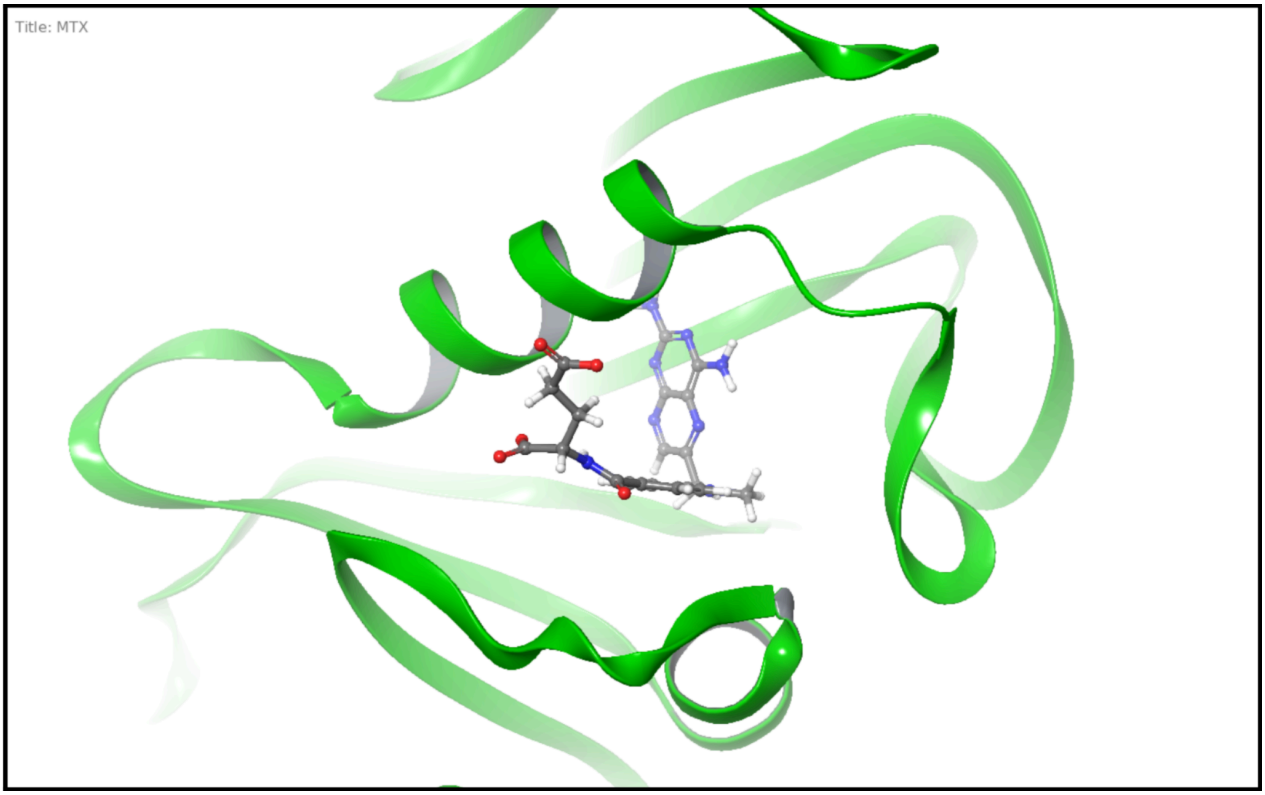

Figure 4. Pose view of methotrexate bound in the DHFR active site. Image created by student researcher using Schrödinger's *Maestro Suite* and Canva, 2025.

2.2 Synthesis of Profluoracil

All chemicals and reagents were purchased from Sigma Aldrich, St. Louis, MO, unless otherwise specified. Based on computational data, profluoracil was selected for synthesis via a Sonogashira cross-coupling reaction, as described by [18], with minimal modifications to quantities and substitutions to chemicals **[see Figure 5]**. In essence, 2 mol% (0.00246 g) tris(dibenzylidenacetone)dipalladium(0), 4 mol% (0.0030 g) triphenylphosphine, 2 mol% (0.00076 g) copper (I) iodide, 2.0 equivalent (34.6 μM) triethylamine, 1.2 equivalent (0.025 g) 5-Fluoro-1-propargyl-uracil, 1.0 equivalent (0.02676 g) 5'-Bromo-2'-Hydroxyacetephenone, and approximately 2.0 mL of DMSO-d_6 were placed into a 5 mL micro reaction vessel under nitrogen to ensure a inert atmosphere **[Figure 6]**. The reaction mixture was stirred for 48 hours at approximately 100 °C, ensuring a steady temperature, and monitored by TLC **[Figure 7]**. Upon completion, the crude product was roughly 3.5 mL in volume. The compound was then characterized by TLC analysis; the calculation of R_f values determined successful completion as plate movement was observed.

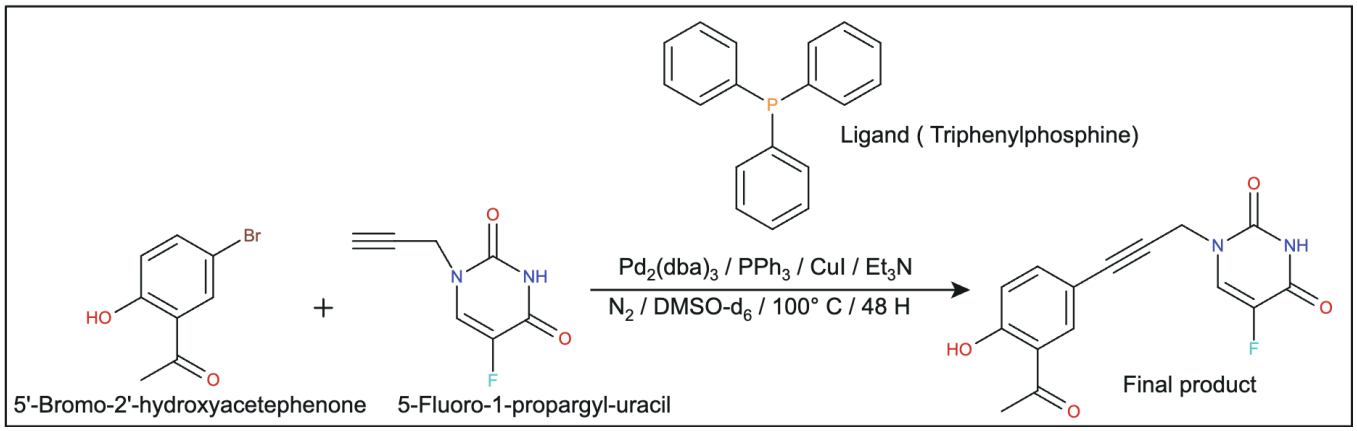

Figure 5. Procedure for the synthesis of profluoracil. Image created by student researcher using Marvin Chemical Drawing, 2025.

.

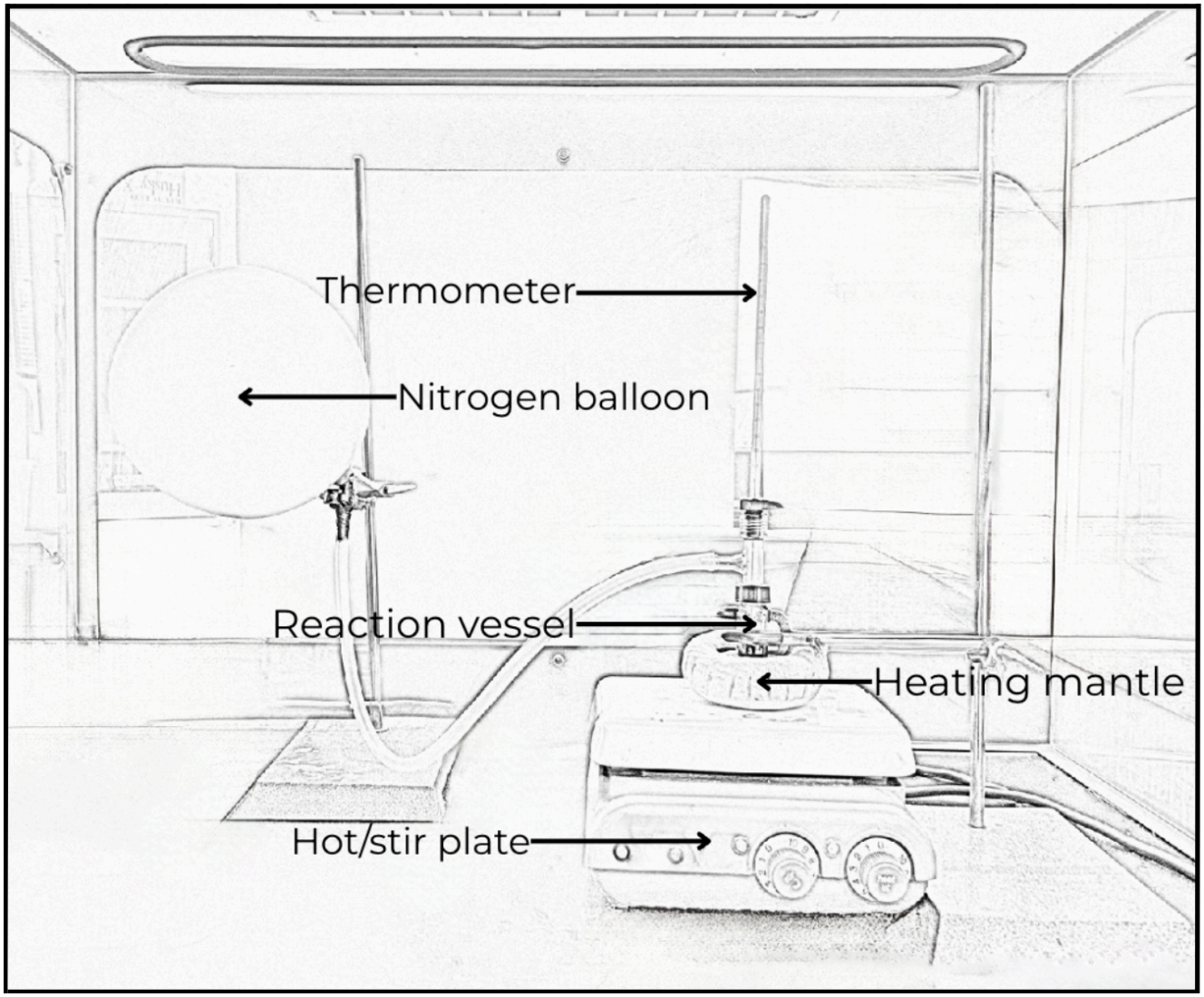

Figure 6. Image of experiment setup. Image created by student researcher in Adobe Photoshop & Canva, 2025.

2.3 Thin Layer Chromatography

Thin-layer chromatography (TLC) was performed on profluoracil at different time intervals throughout the experiment. The mobile phase was 75% Hexane/25% EtOAc. The TLC confirmed loss of initial reactants and formation of new product, indicating successful synthesis of profluoracil.

2.4 Dihydrofolate Reductase Activity Assay

Following the successful synthesis of profluoracil, a *Dihydrofolate reductase* assay kit (Sigma-Aldrich, catalog number CS0340) was performed to quantify the DHFR inhibition by profluoracil relative to a methotrexate control using a recombinant DHFR enzyme. All assay data were analyzed using a UV-1700 PharaSpec Shimadzu UV-Vis Spectrophotometer, with a kinetic program set to 335 nm, running every 5 seconds for 5 minutes at 22°C. Stock solutions of methotrexate and profluoracil at different concentrations were prepared by serial dilution. All stock solutions and reaction reagents were kept on ice, except for the assay buffer. Samples were prepared from 1x assay buffer, DHFR enzyme, NADPH, DHFR acid, and test inhibitors at the ratios/concentrations/volumes listed in **Table 1.** The spectrophotometer measured the absorbance at 335 nm. As DHFR catalyzes the reaction, absorbance at 340 nm decreases. In the presence of an inhibitor, a slower or reduced decrease in absorbance indicates DHFR inhibition.

Reaction	**Assay Buffer (µL)**	**DHFR Enzyme (µL)**	**NADPH (µL)**	**DHFR Acid (µL)**	**Inhibitor (µL)**
Blank 1	980	20	6	–	–
Blank 2	980	20	–	5	–
Reaction 1 (Activity of supplied enzyme)	980	20	6	5	–
Reaction 2A (Inhibition by **100 µM** Methotrexate)	980	20	6	5	10
Reaction 2B					

(Inhibition by **10 µM** Methotrexate)	980	20	6	5	10
Reaction 2C (Inhibition by **1 µM** Methotrexate)	980	20	6	5	10
Reaction 3A (Inhibition by **10 µM** profluoracil)	980	20	6	5	10
Reaction 3B (Inhibition by **5 µM** profluoracil)	980	20	6	5	10
Reaction 3C (Inhibition by **1 µM** profluoracil)	980	20	6	5	10
Reaction 3D (Inhibition by **0.1 µM** profluoracil)	980	20	6	5	10
Reaction 3E (Inhibition by **0.01 µM** profluoracil)	980	20	6	5	10
Reaction 3F (Inhibition by **0.005 µM** profluoracil)	980	20	6	5	10

Table 1. Reaction scheme for ratios, concentrations, and volumes of DHFR activity detection and DHFR activity inhibition for both methotrexate and profluoracil. Image created by student researcher in Google Docs, 2025.

2.5 Cytotoxicity Assay

Profluoracil was tested for antimicrobial activity compared to a methotrexate control. Both profluoracil and methotrexate were tested against *Escherichia coli* suspended in broth. Using a previously created *E. coli* culture, a small amount of growing *E. coli* was placed into broth and incubated in a water bath at 37°C for 18 hours to promote bacterial growth. Dilutions of 100 μM MTX, 10 μM MTX, 1 μM MTX, 1000 μM profluoracil, 500 μM profluoracil, 100 μM profluoracil, 10 μM profluoracil, 1 μM profluoracil, and 0.1 μM profluoracil were created, and 100 μL of each was added to 8 different microcentrifuges filled with 600 μL of the 18-hour cultured broth, respectively. These microcentrifuges were incubated in a water bath at 37°C for 20 hours. Using a Vernier SpectroVis Plus Spectrophotometer connected to LoggerPro, the OD600 (optical density at 600 nm) was measured to determine the solution's turbidity and assess whether the bacteria survived. First, a blank-cuvette calibration with water was performed to prepare the instrument. Then, 700 μL of each bacterial microcentrifuge solution containing both methotrexate and profluoracil was added to different curved cuvettes, which were then placed into the instrument. The optical density of each microcentrifuge containing different concentrations was measured in the spectrophotometer to assess toxicity.

3 Results

3.1 Computational Data

Results from computational testing represent both known (UCP1162, trimethoprim) and discovered (profluoracil, probromoben, promethylacetephen, probromoacetephen) nonclassical inhibitors in terms of glide docking score, predicted value for blockage of HERG K^+ channels (QPlogHERG), and predicted human oral absorption (PercentHumanOralAbsorption) **[Table 2]** [19]. The ligand interaction diagrams for each compound **[Table 3]** reveal specific interactions between the ligand's position in hDHFR's cavity. Profluoracil was selected for synthesis due to its exceptional docking performance, straightforward synthesis, relative toxicity, and % oral absorption when compared to other candidates. A lower docking score is optimal, and profluoracil significantly outperformed the other two candidates. Additionally, regarding toxicity, profluoracil outperformed

UCP1162; however, it falls slightly below the margin of concern, as values below -5 are considered troublesome. In terms of absorption, values above 80 are considered high; thus, 75% profluoracil is predicted to be acceptable.

Compound (Known)	**Docking Score**	**QPlogHERG**	**%HumanOralAbsorption**
Trimethoprim	-6.524	-4.180	77.073
UCP1162	-8.578	-6.281	84.065
Compound (Discovered)	**Docking Score**	**QPlogHERG**	**%HumanOralAbsorption**
Profluoracil	-10.654	-5.056	75.299
Probromobenzene	-10.146	-6.487	89.708
Promethylacetephen	-10.045	-5.074	86.167
Probromoacetephen	-9.983	-5.046	83.056

Table 2. Computational results of discovered and known candidates; Green = exceptional results, yellow = cautionable results, red = poor results compared to various nonclassicals. QPlogHERG > -5 is ideal, > 80% absorption is high, while < 25% is poor; orange = selected compound. Created by student researcher using Google Docs, 2025.

Trimethoprim	**UCP1162**

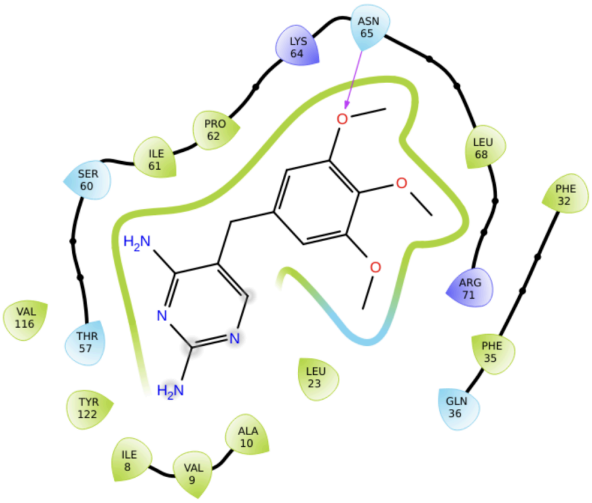

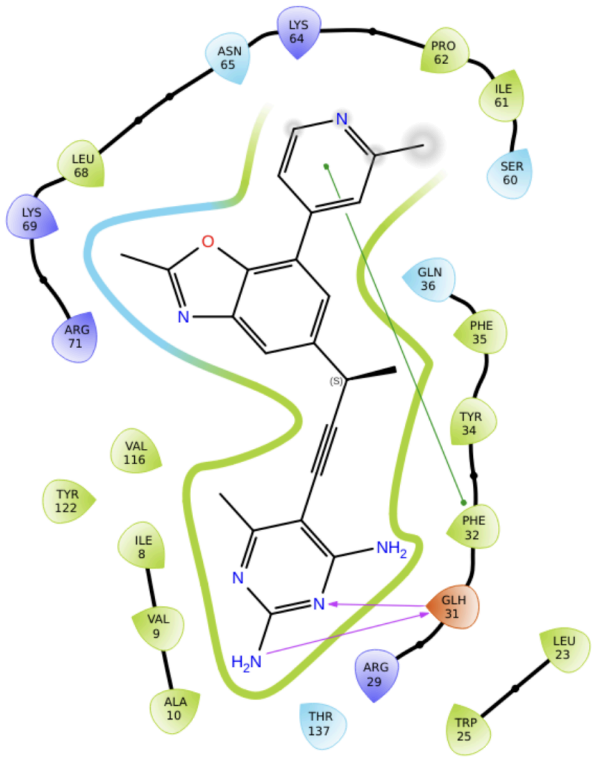

Profluoracil

Probromobenzene

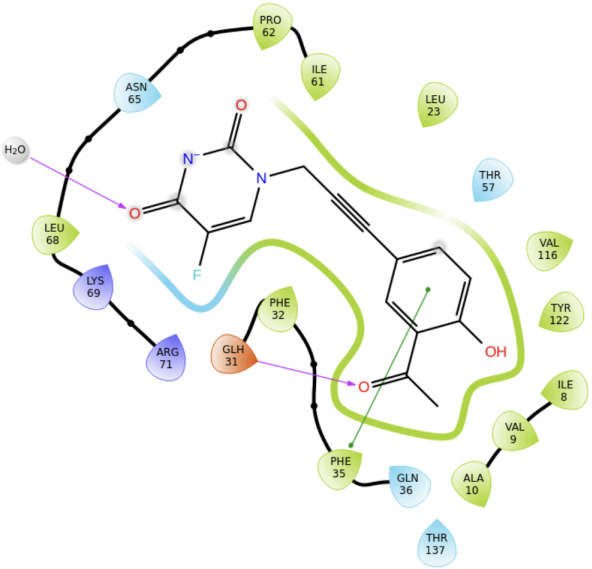

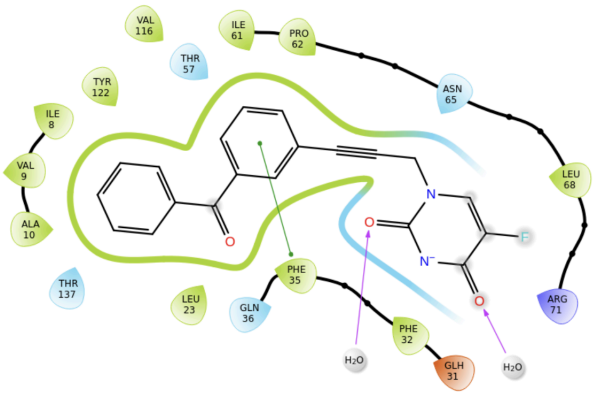

Promethylacetephen	Probromoacetephen
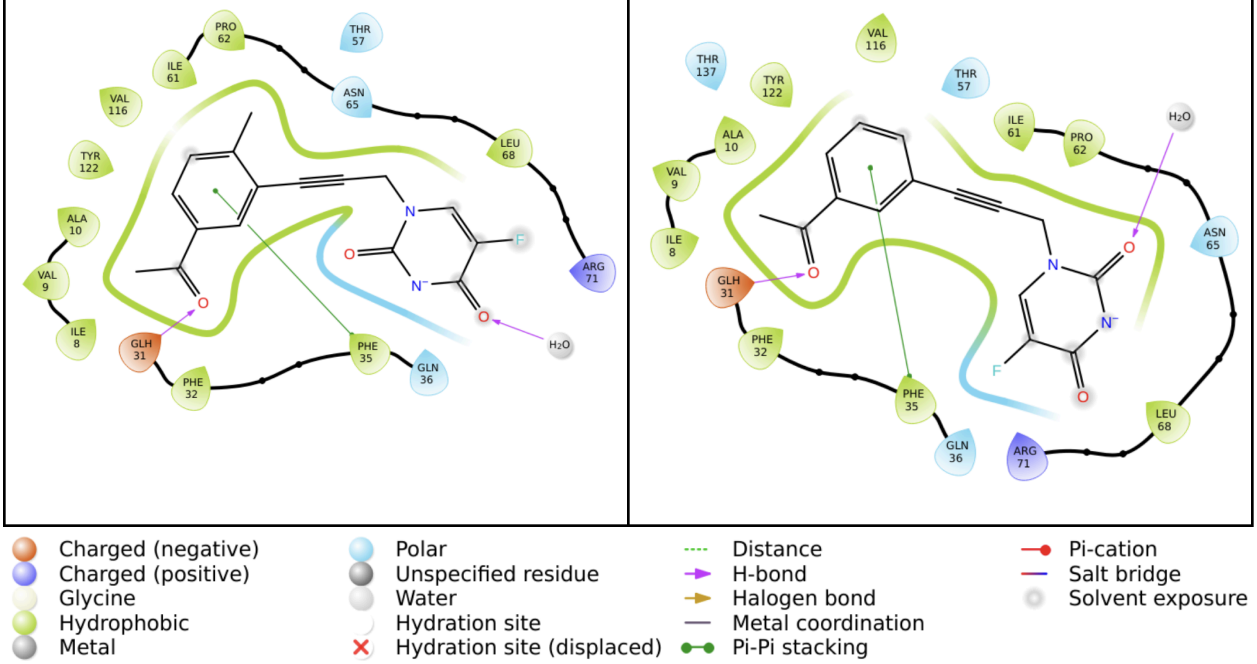	

Table 3. Ligand interaction diagrams of known and discovered compounds. Created by student researcher using Schrödinger's *Maestro Suite*, 2025.

3.2 TLC Data from Synthesis

Reaction progress was monitored by Thin-Layer Chromatography, which showed the disappearance of the starting reactants and the emergence of the product, with distinct R_f values. The appearance of this product indicates successful synthesis of profluoracil under the chosen reaction conditions.

3.3 DHFR Activity Assay Data

The percentage of relative inhibition was calculated using: % relative inhibition = (slope of enzyme-slope of sample/slope of enzyme)*100. Inhibition is the percent decrease in activity of the enzyme when the drug is present. The percentage of inhibition for 10 μM, 5 μM, 1 μM, 0.1 μM, 0.01 μM, and 0.005 μM was calculated to be 85%, 86%, 96%, 80%, 93%, and 85% respectively.

Profluoracil exhibits nanomolar range inhibition, reaching a peak inhibition of 85% **[Figure 7].** The slope was calculated according to the equation ([EC]- [S])/[EC] * 100. [EC]= Slope of Enzyme control: original slope = uninhibited enzyme activity - slope of activity without DHFR acid. [S]= Slope of the sample: slope of sample - slope of activity without DHFR acid (ex.,100 μM methotrexate).

Sample calculation:

[EC] = -0.000369767 - ($-1.4303*10^{-5}$) = $-3.55464*10^{-4}$

[S] = $-6.84462*10^{-5}$ - ($-1.4303*10^{-5}$) = $-5.41432*10^{-5}$ (Slope of 10 μM profluoracil)

Percent inhibition = ($-3.55464*10^{-4}$) - ($-5.41432*10^{-5}$)/($-3.55464*10^{-4}$) * 100

Percent inhibition 10 μM profluoracil = 85 %

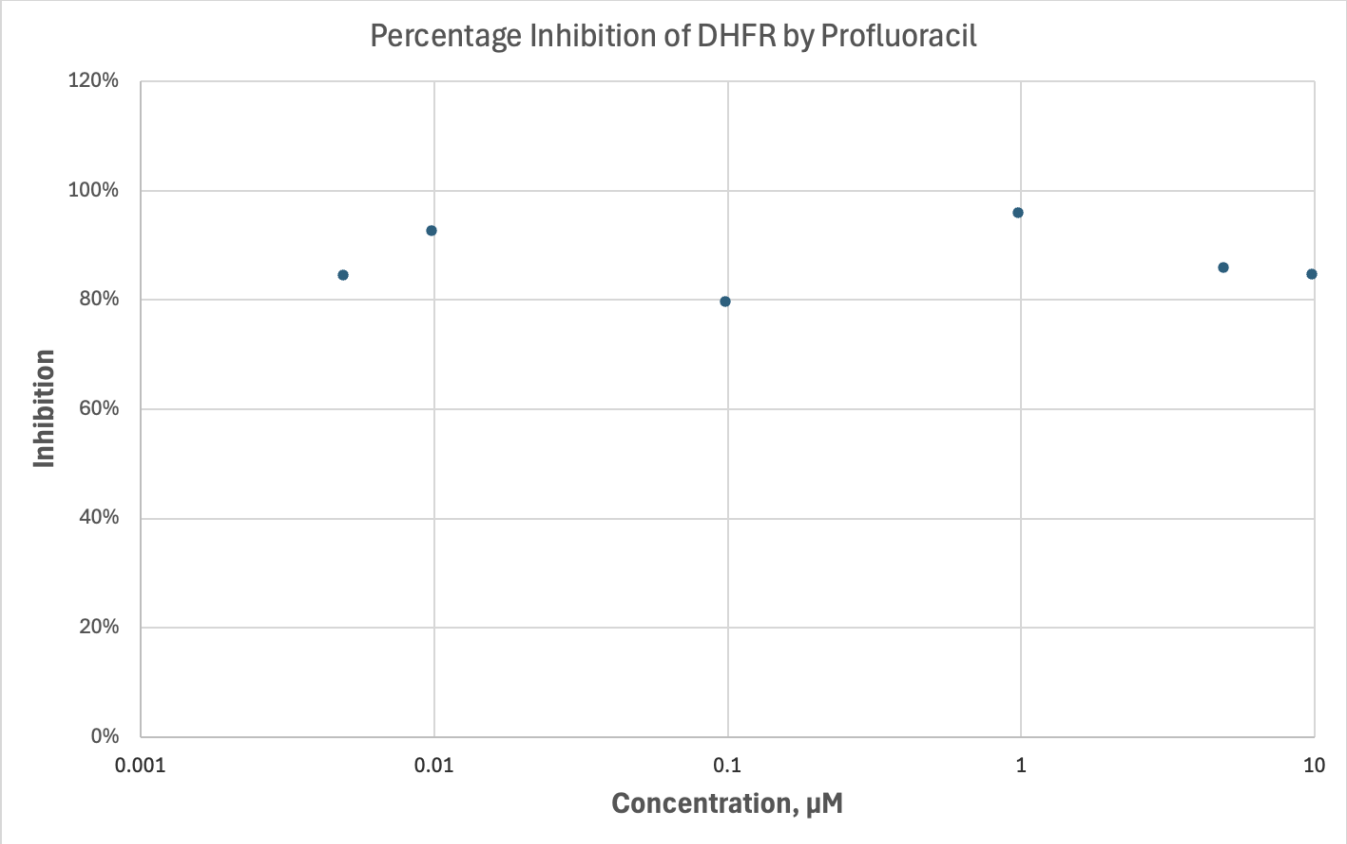

Figure 7. Percentage inhibition of Profluoracil at different concentrations. Image created by student researcher using Excel, 2025.

3.4 Cytoxicity Assay Data

Results from antimicrobial testing indicate that profluoracil exhibits lower cytotoxicity—effective in the nanomolar to micromolar range—than methotrexate. OD600 values for different concentrations of both methotrexate and profluoracil **[Figure 8]**. The reference absorbance was 0.759 nm; if the drug were not harmful to the living bacteria, the absorbance would be higher because there would be greater turbidity, indicating more bacteria. Profluoracil showed no toxic effects on bacterial growth at 600.3 nm at all concentrations, expressing its potential as a less toxic therapeutic agent.

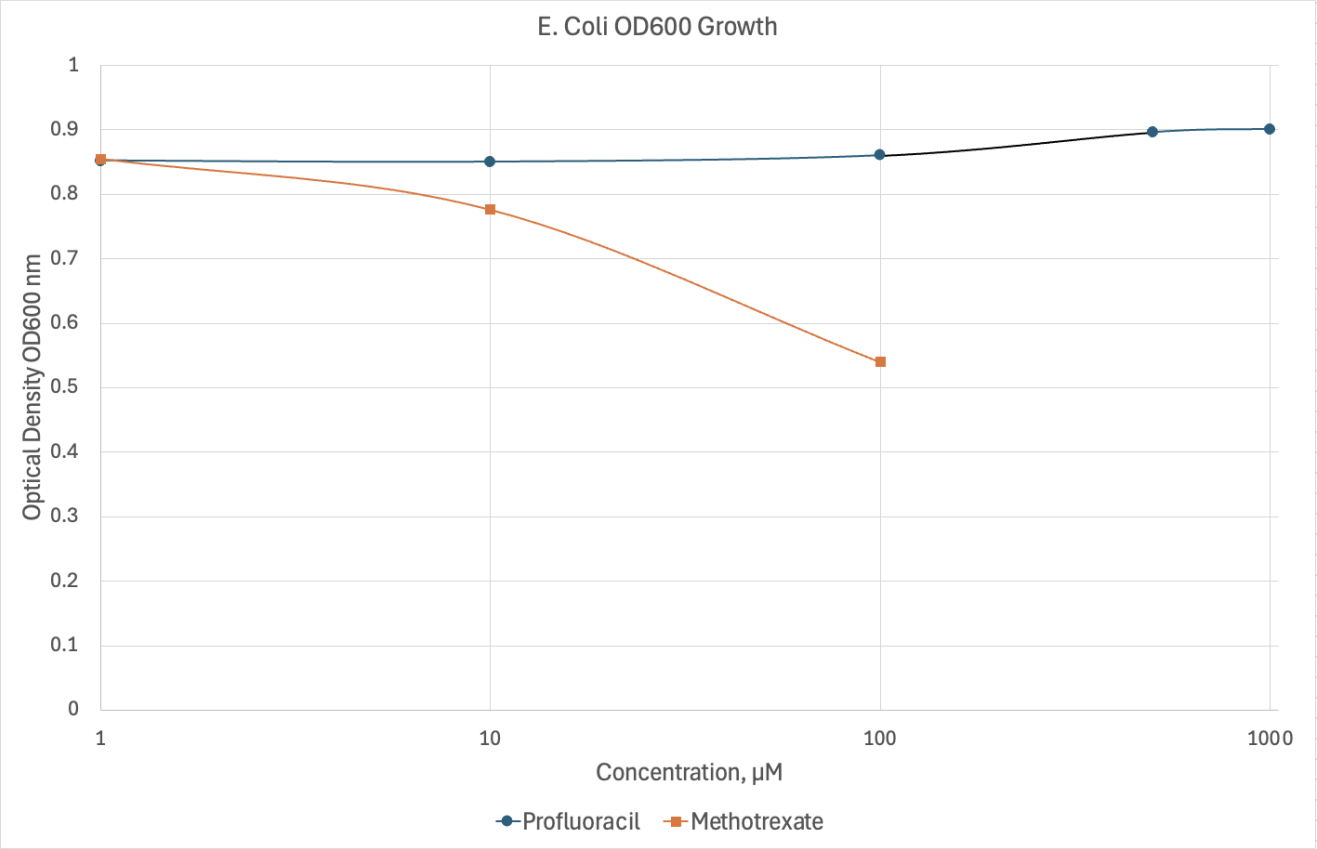

Figure 8. A graph of the absorbance (OD600) vs concentration dosed with methotrexate (orange square line) and profluoracil (blue circle line). Image created by student researcher using Excel, 2025.

4 Discussion

Profluoracil was successfully synthesized in a one-step process using commercially available reagents and Sonogashira cross-coupling, offering high yield and reliability.

In initial testing, profluoracil shows inhibition data in the nanomolar range, indicating potency comparable to or possibly even exceeding that of the current drugs of choice, such as methotrexate and pemetrexed, which have median IC_{50} values of approximately 78 nM and 155 nM, respectively [20]. Further testing is needed to clearly determine the IC_{50} of profluoracil; however, inhibition >85% was observed at 5 nM.

Additionally, initial antimicrobial testing suggests that proflouracil exhibits lower toxicity than methotrexate. When profluoracil was tested at low micromolar to high nanomolar concentrations against a growing *E. coli* culture, no inhibitory effects on growth were observed, indicating minimal toxicity. OD600 measurements, which reflect the density of microbial cells in a liquid culture, showed increased absorbance following treatment. The higher optical density measurement indicated that more light was scattered due to the higher cell density, confirming that profluorical did not negatively affect bacterial growth.

Profluoracil's structure inherently differs from the common folate and purine-like structure of existing antifolates. However, the fluorinated uracil scaffold enhances hydrogen bonding and pi-pi stacking interactions within the DHFR active site. As a result, profluoracil is a potent dihydrofolate reductase inhibitor in humans, with inhibitory activity comparable to that of methotrexate and superior to that of existing nonclassical treatments.

Additional propargyl-linked uracil-based scaffolds were tested in Schrödinger and are predicted to have affinities and toxicities comparable to profluoracil. These compounds (scores and structures shown in **Table 2 and Table 3**) were screened against hDHFR in the same manner as profluoracil, but could not be synthesized due to resource constraints. However, if synthesized, each could exhibit potency and toxicity similar to that of profluoracil, suggesting the potential for additional high-performing fluorinated-uracil DHFR inhibitors.

These findings are based on initial computational and modeling analyses; additional enzymatic and cytotoxicity assays would confirm efficacy. The likelihood that profluoracil would be subject to similar cellular resistance issues as those seen with common antifolates is an area for future

investigation. Studies evaluating its transport mechanisms and efflux sensitivity could provide a comprehensive understanding of the compound's resistance profile relative to methotrexate. In the context of psoriasis, a selective, less toxic DHFR inhibitor such as profluoracil could minimize side effects while increasing efficacy. Further research should include cellular studies to confirm these properties and develop profluoracil as the future of nonclassical DHFR inhibition.

5 Limitations and Future Directions

Out of the ~12 compounds that were successfully identified to be promising candidates, only one could be synthesized with commercially available reagents. The synthesis of additional uracil-based compounds offers the potential to develop less toxic and more effective antifolate candidates. Characterization of profluoracil by Carbon NMR or Fourier Transform Infrared Spectroscopy would have provided another and more concrete method of the compound's characterization. Additionally, the further purification of profluoracil by rotary evaporation and chromatography would be beneficial for purifying the drug candidate rather than relying on the crude product. In terms of testing, access to more DHFR enzyme would have enabled further testing of profluoracil's effectiveness against DHFR, allowing evaluation at lower concentrations and the generation of an IC_{50} curve. In vivo testing in psoriasis-infected mammalian models would demonstrate the drug's toxicity and the progression of the disease in a living model, while an MTS viability assay would have enabled the determination of an EC_{50} value, thereby quantifying the cytotoxic effect of profluoracil; however, this was not possible in the current research setting. Additionally, cellular proliferation assays could have been used to quantify cell division and measure the metabolic activity of live cells, which was also not possible in the current research setting.

6 Conclusion

This project demonstrated the successful discovery, synthesis, and evaluation of profluoracil, a small molecule dihydrofolate reductase (DHFR) inhibitor designed for psoriasis treatment. The compound was assessed for DHFR inhibition and antimicrobial properties, with cytotoxicity data indicating reduced toxicity against microbial strains and DHFR activity data demonstrating significant inhibitory potency against human DHFR. The compound's smaller, nonclassical structure

provided a straightforward synthesis while maintaining increased efficacy. Structural and computational analysis revealed that the fluorinated uracil scaffold and propargyl linker allowed the compound to extend into DHFR's hydrophobic pocket, forming strong hydrogen bonding and hydrophobic interactions with key residues (VAL116, TYR122, ILE8). These properties contribute to the exceptional docking score (-10.654) and favorable pharmacokinetic properties, including QPlogHERG and %HumanOralAvalbility scores (-5.056 and 75.299, respectively). Together, these findings demonstrate profluoracil as a promising scaffold for the future of DHFR inhibition, and given DHFR's central role in cellular proliferation, profluoracil could hold promise not only for psoriasis treatment but also for the treatment of autoimmune and cancer diseases.

Acknowledgements

This project would not have been possible without the dedication and mentorship of **Dr. Timothy Anglin** and **Dr. Michael Bruno**, the supplies and guidance of **Mr. Antonio Lopez**, the support and motivation of **My Research in Chemistry Peers and Luke Malta**, the financial support for my project from the **NCSSM Foundation**, the support and excitement from the **NCSSM Science Department**, and **Dr. Heather Mallory** for the biology related questions.

References

[1] Garg, S.; Dixit, M.; Malhotra, I.; Singh, M.; Singh, V. From Manifestations to Innovations: A Deep Dive into Psoriasis, its Clinical Diversity, Conventional Treatments, and Emerging Therapeutic Paradigms. *International Immunopharmacology* **2024**, *143*, 113508. DOI: https://doi.org/10.1016/j.intimp.2024.113508

[2] Kim, G. K.; Del Rosso, J. Q. Drug-Provoked Psorasis: Is It Drug Induced or Drug Aggravated?: Understanding Pathophysiology and Clinical Relevance. *The Journal of Clinical and Aesthetic Dermatology* **2010** *3* (1) 32–38. Available from: https://pmc.ncbi.nlm.nih.gov/articles/PMC2921739/ (accessed June 15, 2025).

[3] Orzit-Lopez, L.; Choudhary, V.; Bollag, W. B. Updated Perspectives on Keratinocytes and Psoriasis: Keratinocytes are More Than Innocent Bystanders. *Psoriasis* **2022**, *12*, 73–87. DOI: https://doi.org/10.2147/PTT.S327310

[4] Yap, S. M.; Bonsall, A. Psoriasis. *Medicine* **2025**, *53* (7) 441–447 DOI: https://doi.org/10.1016/j.mpmed.2025.04.019

[5] Raimondi, M. V.; Randazzo, O.; La Franca, M.; Barone, G.; Vignoni, E.; Rossi, D.; Collina, S. DHFR Inhibitors: Reading the Past for Discovering Novel Anticancer Agents. *Molecules* **2019**, *24* (6) 1140. DOI: https://doi.org/10.3390/molecules24061140

[6] The Wednesday Island. *Psoriasis of the Back.* **2006.** Wikipedia. Licensed under GNU Free Documentation License (GFDL). https://commons.wikimedia.org/wiki/File:Psoriasis_on_back.jpg

[7] Tezgin, D. O.; Kurkcu, S.; Si, D.; Krucinska, J.; Mosley, A.; Mehta, P.; Babic, I.; Nurmemmedov, E.; Kuo, A.; He, W.; Nelson, C. E.; Wright, L.; Wright, D. L.; Giardina, C. Evaluation of UCP1162, a Potent Propargyl-Linked Inhibitor of Dihydrofolate Reductase with Potential Application to Cancer and Autoimmune Disease. *Biochemical Pharmacology* **2024**, *230*, 116617. DOI: https://doi.org/10.1016/j.bcp.2024.116617

[8] Algul, O.; Paulsen, J. L.; Anderson, A. C. 2,4-Diamino-5-(2'-arylpropargyl)pyrimidine Derivatives as New Nonclassical Antifolates for Human Dihydrofolate Reductase

Inhibition. *Journal of Molecular Graphics and Modeling* **2011**, *29* (5), 608–613. DOI: https://doi.org/10.1016/j.jmgm.2010.11.004

[9] Gao, T.; Zhang, C.; Shi, X.; Guo, R.; Zhang, K.; Gu, J.; Li, L.; Li, S.; Zheng, Q.; Cui, M.; Gao, X.; Liu, Y.; Wang, L. Targeting Dihydrofolate Reductase: Design, Synthesis, and Biological Evaluation of Novel 6–Substituted Pyrrolo[2,3-*d*]pyrimidines as Nonclassical Antifolates and as Potential Antitumor Agents. *European Journal of Medicinal Chemistry* **2019**, *178*, 329–340. DOI: https://doi.org/10.1016/j.ejmech.2019.06.013

[10] Friedman, B.; Cronstein, B. Methotrexate Mechanism in Treatment of Rheumatoid Arthritis. *Joint Bone Spine* **2019**, *86* (3), 301–307. DOI: https://doi.org/10.1016/j.jbspin.2018.07.004

[11] Rana, R. M.; Rampogu, S.; Bin Abid, N.; Zeb, Amir.; Parate, S.; Lee, G.; Yoon, S.; Kim, Y.; Kim, D.; Woo Lee, K. In Silico Study Identified Methotrexate Analog as Potential Inhibitor of Drug Resistant Human Dihydrofolate Reductase for Cancer Therapies. *Molecules* **2020**, *25* (15), 3510. DOI: https://doi.org/10.3390/molecules25153510

[12] Katturajan, R.; Viajayalakshmi, S.; Rasool, M.; Prince, S. E. Molecular Toxicity of Methotrexate in Rheumatoid Arthritis Treatment: A Novel Perspective and Therapeutic Implications. *Toxicology* **2021**, *461*, 152909. DOI: https://doi.org/10.1016/j.tox.2021.152909

[13] Serra, M.; Branchat-Reverter, G.; Maurici, D. Benini, S.; Shen, J. N.; Chano, T.; Hattinger, C. M.; Manara, M. C.; Pasello, M.; Scotlandi, K.; Picci, P. Analysis of Dihydrofolate Reductase and Reduced Folate Carrier Gene Status in Relation to Methotrextae Resistance in Osteosarcoma Cells. *Official Journal of the European Society for Medical Oncology* **2004**, *15* (1), 151–160. DOI: https://doi.org/10.1093/annonc/mdh004

[14] Reeve, S. M.; Scocchera, E.; Ferreira, J. J.; G-Dayanandan, N.; Keshipeddy, S.; Wright, D. L.; Anderson, A. C. Charged Propargyl-Linked Antifolates Reveal Mechanisms of Antifolate Resistance and Inhibit Trimethoprim-Resistant MRSA Strains Possessing Clinically Relevant Mutations. *Journal of Medicinal Chemistry* **2016**, *59* (13), 6493–6500. DOI: https://doi.org/10.1021/acs.jmedchem.6b00688

[15] Wróbel, A.; Arciszawska, K.; Maliszewski, D.; Drozdowska, D. Trimethoprim and Other Nonclassical Antifolates an Excellent Template for Searching Modifications of Dihydrofolate Reductase Enzyme Inhibitors. *The Journal of Antibiotics* **2019**, *73* (1), 5–27. DOI: https://doi.org/10.1038/s41429-019-0240-6

[16] Reeve, S. M.; Scocchera, E.; Ferreira, J. J.; G-Dayanandan, N.; Keshipeddy, S.; Wright, D. L.; Anderson, A. C. Charged Propargyl-Linked Antifolates Reveal Mechanisms of Antifolate Resistance and Inhibit Trimethoprim-Resistant MRSA Strains Possessing Clinically Relevant Mutations. *Journal of Medicinal Chemistry* **2016**, *59* (13), 6493–6500. DOI: https://doi.org/10.1021/acs.jmedchem.6b00688

[17] Scocchera, E.; Reeve, S. M.; Keshipeddy, S.; Lombardo, M. N.; Hajian, B.; Sochia, A. E.; Alverson, J. B.; Priestley, N. D.; Anderson, A. C.; Wright, D. L. Charged Nonclassical Antifolates with Activity Against Gram–Positive and Gram–Negative Pathogens. *ACS Medicinal Chemistry Letters* **2016**, *7* (7), 692–696. DOI: https://doi.org/10.1021/acsmedchemlett.6b00120

[18] Mino, T.; Suzuki, S.; Hirai, K.; Sakamoto, M.; Fujita, T. Hydrazone-Promoted Sonogashira Coupling Reaction with Aryl Bromides at Low Palladium Loadings. *Synlett* **2011** (9), 1277–1280. DOI: https://doi.org/10.1055/s-0030-1260535

[19] Schrödinger, LLC. *QikProp 4.4 User Manual*. Schrödinger, LLC. New York, NY, 2015.

[20] Norris, R. E.; Adamson, P. C. Clinical Potency of Methotrexate, Aminopterin, Talotrexin, and Pemetrexed in Childhood Leukemias. *Cancer Chemotherapy and Pharmacology* **2010**, *65* (6), 1125–1130. DOI: https://doi.org/10.1007/s00280-009-1120-8